Precise Response Control of Transmit-Receive Two-Dimensional Beampattern in FDA-MIMO Radar

1st Lan Lan
National Lab of Radar Signal Processing
Xidian University
Xi'an, China
lanlan_xidian@foxmail.com

2nd Jingwei Xu
National Lab of Radar Signal Processing
Xidian University
Xi'an, China
xujingwei1987@163.com

3rd Guisheng Liao
National Lab of Radar Signal Processing
Xidian University
Xi'an, China
liaogs@xidian.edu.cn

4th Yuhong Zhang
School of Electronic Engineering
Xidian University
Xi'an, China
yuhzhang@xidian.edu.cn

5th Yan Huang
State Key Laboratory of Millimeter Waves
Southeast University
Nanjing, China
yellowstone0636@hotmail.com

***Abstract*—Frequency diverse array (FDA) has sparked intense interest in recent years because of its range-angle-dependent beampattern. By combining with the multiple-input and multiple-output (MIMO) technique, additional degrees of freedom (DOFs) are provided. However, dynamic environments require the design of a precisely controlled beampattern to enhance the robustness of the radar system. In this paper, the precise response control (PRC) algorithm is studied in the FDA-MIMO radar by imposing artificial interferences within rectangular regions in the joint transmit-receive spatial frequency domain. The algorithm is performed via two stages. In the first stage, artificial interferences are concurrently imposed to iteratively adjust the responses. In the second stage, extra artificial interferences are added to satisfy the predefined response requirement for all regions. The jammer-plus-noise covariance matrix is constructed accordingly and the weight vector is updated. Particularly, the jammer-to-noise ratio (JNR) of each artificial interference is figured out. Numerical results are provided to corroborate the performance of the transmit-receive two-dimensional beampattern in FDA-MIMO.**

***Index Terms*—FDA-MMO radar, artificial interference, two-dimensional beampattern, rectangular regions, jammer-plus-noise covariance matrix, joint transmit-receive spatial frequency domain**

I. Introduction

Beamforming techniques for antenna arrays have been widely investigated. To improve the system performance and enhance the robustness, a host of applications ranging from radar and navigation to wireless communication systems require the design of a desired beampattern [1]. Particularly, dynamic environments where the range and angle of the interference are time-varying arouse the need for broadened nulls to adequately suppress the moving interferences. Moreover, it is necessary to mitigate returns from interfering signals by designing a beampattern with low sidelobe level.

Over the last several decades, significant attention has been paid to pattern synthesis. By iteratively minimizing the deviation between the synthesized and desired patterns, the beampattern is adjusted using the adaptive array theory [2,3]. However, parameter selection needs further investigation. Methods based on intelligent optimization algorithms [4-6] use stochastic approaches to design the beampattern. However, they suffer from high computational complexity. Optimization methods such as semidefinite relaxation (SDR) was applied to pattern synthesis [7]. Nevertheless, the resultant beampattern cannot be controlled precisely since the relaxation leads to an approximate solution. Moreover, a systematic approach was presented in [8] by imposing artificial interferers in sidelobes. However, the powers of artificial interferences are selected in an *ad hoc* way. In [9], the optimal and precise array response control (OPARC) algorithm was proposed and a new formulation of the weight vector was devised.

Notably, these methods to preciously control the beampattern were developed based on the phased array. The frequency diverse array (FDA) has been widely investigated during the past few years [10-12]. It can generate a range-angle-time-dependent beampattern by utilizing a small frequency increment across array elements. The advantages of FDA over the traditional phased array have been extensively explored in the literatures [13,14]. By combining with the multiple-input and multiple-output (MIMO) technique, the FDA-MIMO radar provides more degrees of freedom (DOFs) and has found an immense utilization [15-17]. Although many efforts have been devoted to FDA-MIMO radar, existing works do not take into account the robustness issue frequently encountered in practice.

Adaptive beamformers can extract the signal of interest (SOI) while suppressing interferences by adjusting the weight

978-9-0827-9703-9/19/$31.00 ©2019 IEEE

vector according to the environment. However, sufficient training samples are needed to estimate the jammer-plus-noise covariance matrix and the performance will degrade if they are no longer independent and identically distributed. Data-independent beamforming is defined by forming a fixed spatial directivity pattern at a particular point. It is easy to implement without samples. Thus, the data-dependent adaptive array theory can be applied into a data-independent situation.

In this paper, the precise response control (PRC) algorithm is proposed to control the transmit-receive two-dimensional (2-D) beampattern in FDA-MIMO radar. Multiple artificial interferences are assigned within a prescribed rectangular region in the joint transmit-receive spatial frequency domain. Subsequently, the jammer-plus-noise covariance matrix is constructed. This allows us to optimally update the weight vector to achieve the given response. Specifically, the jammer-to-noise ratio (JNR) of each artificial interference is figured out. Notably, the jammer-plus-noise covariance matrix has no physical meaning since it is obtained with artificial interferences instead of real samples.

The remainder of this paper is organized as follows. Section II presents the transmit-receive 2-D beampattern in FDA-MIMO radar. The PRC method to precisely control the 2-D beampattern is explored in Section III. Simulation results and performance analysis are given in Section IV. Conclusions are drawn in Section V.

Notations: $j \triangleq \sqrt{-1}$. Boldfaced lowercase letters such as $\boldsymbol{x}$ represent a vector, and boldfaced uppercase letters, such as $\boldsymbol{A}$, denote a matrix. For the vector $\boldsymbol{x}$, we use $[\boldsymbol{x}]_n$ to denote the n-th component of vector $\boldsymbol{x}$. For the matrix $\boldsymbol{A}$, we use $[\boldsymbol{A}]_{m,n}$ to denote the component of $\boldsymbol{A}$ in the m-th row and the n-th column, $[\boldsymbol{A}]_{m,:}$ to denote the m-th row vector of $\boldsymbol{A}$ and $[\boldsymbol{A}]_{:,n}$ to denote the n-th column vector of $\boldsymbol{A}$. $\boldsymbol{I}_N$ denotes a $N \times N$ identity matrix. $|\cdot|$ denotes the absolute value. The transpose and conjugate transpose of a matrix or vector are denoted by $(\cdot)^{\mathrm{T}}$ and $(\cdot)^{\dagger}$ respectively. $\otimes$ denotes the Kronecker product. The symbols $\mathbb{C}$ and $\mathbb{N}^{+}$ are the complex space and the positive integer space, respectively. $\mathrm{diag}\{\cdot\}$ denotes the diagonal matrix.

II. Transmit-receive 2-D beampattern in FDA-MIMO radar

We consider a colocated FDA-MIMO radar system which consists of M transmit elements and N receive elements with half-wavelength inter-element distance. The carrier frequency increases linearly across the aperture with a small frequency increment Δf, and the carrier frequency of the m-th ($m = 1, 2, \cdots, M$) element is written as

$$f_m = f_0 + (m-1)\Delta f, \tag{1}$$

where f_0 is the reference carrier frequency. Given a far-field point target at the angle θ_0 and range R_0, the round-trip propagation time delay from the m-th transmit element to the n-th ($n = 1, 2, \cdots, N$) receive element is expressed as

$$\tau_{m,n} = \tau_0 - \frac{d\,(n-1)\sin(\theta_0) + d\,(m-1)\sin(\theta_0)}{c}, \tag{2}$$

where c is the speed of light, $\tau_0 = \frac{2R_0}{c}$, d is the inter-element spacing. Under the assumption of a narrowband, the signal received by the n-th element is expressed as

$$\begin{aligned} &y_n(t-\tau_0) \approx \alpha \sum_{m=1}^{M} x_m(t-\tau_0)\exp\{j2\pi f_m(t-\tau_{m,n})\} \\ &= \alpha \exp\{j2\pi f_0(t-\tau_0)\}\exp\{j\pi(n-1)\sin(\theta_0)\} \\ &\cdot \sum_{m=1}^{M} x_m(t-\tau_0)\exp\{j2\pi\Delta f(m-1)(t-\tau_0)\} \\ &\quad \cdot \exp\{j\pi(m-1)\sin(\theta_0)\}, \end{aligned} \tag{3}$$

where α is the complex-valued coefficient of the point source and $x_m(t)$ is the m-th transmitted waveform. The complex envelopes are assumed to be orthogonal to each other, i.e., $\int_{T_p} x_{m'}(t)\, x_m^*(t-\tau) = 0, m \neq m', \forall \tau$ with T_p being the radar pulse duration and τ being an arbitrary time delay. After matched filtered with $x_m(t-\tau_0)\exp\{j2\pi f_m t\}$ and stacking the output vector from N receive elements, the received signal is decomposed as

$$\boldsymbol{x}_s = \xi_{\mathrm{S}} \boldsymbol{b}(f_{\mathrm{R}}^{\mathrm{S}}) \otimes \boldsymbol{a}\left(f_{\mathrm{T}}^{\mathrm{S}}\right), \tag{4}$$

where ξ_{S} denotes the equivalent coefficient of the target [17], $f_{\mathrm{T}}^{\mathrm{S}}$ and $f_{\mathrm{R}}^{\mathrm{S}}$ denote the transmit and receive spatial frequencies, which are expressed as

$$f_{\mathrm{T}}^{\mathrm{S}} = -\Delta f \frac{2R_0}{c} + \frac{1}{2}\sin(\theta_0), \tag{5a}$$

$$f_{\mathrm{R}}^{\mathrm{S}} = \frac{1}{2}\sin(\theta_0), \tag{5b}$$

$\boldsymbol{a}\left(f_{\mathrm{T}}^{\mathrm{S}}\right) \in \mathbb{C}^{M\times 1}$ and $\boldsymbol{b}\left(f_{\mathrm{R}}^{\mathrm{S}}\right) \in \mathbb{C}^{N\times 1}$ represent the transmit and receive steering vectors, respectively, and they have the forms of

$$\boldsymbol{a}\left(f_{\mathrm{T}}^{\mathrm{S}}\right) = \left[1, e^{j2\pi f_{\mathrm{T}}^{\mathrm{S}}}, \cdots, e^{j2\pi(M-1)f_{\mathrm{T}}^{\mathrm{S}}}\right]^{\mathrm{T}}, \tag{6a}$$

$$\boldsymbol{b}\left(f_{\mathrm{R}}^{\mathrm{S}}\right) = \left[1, e^{j2\pi f_{\mathrm{R}}^{\mathrm{S}}}, \cdots, e^{j2\pi(N-1)f_{\mathrm{R}}^{\mathrm{S}}}\right]^{\mathrm{T}}. \tag{6b}$$

It follows the normalized transmit-receive 2-D beampattern in the joint transmit-receive spatial frequency domain as

$$\begin{aligned} &P(f_{\mathrm{T}}, f_{\mathrm{R}}) = \frac{\boldsymbol{u}_{\mathrm{S}}^{\mathrm{H}}}{MN}\boldsymbol{u} \\ &= \left[\frac{1}{M}\boldsymbol{a}^{H}\left(f_{\mathrm{T}}^{\mathrm{S}}\right)\boldsymbol{a}(f_{\mathrm{T}})\right] \otimes \left[\frac{1}{N}\boldsymbol{b}^{H}\left(f_{\mathrm{R}}^{\mathrm{S}}\right)\boldsymbol{b}(f_{\mathrm{R}})\right] \\ &= \left[\frac{1}{M}\frac{\sin\left(\pi M\left(f_{\mathrm{T}}-f_{\mathrm{T}}^{\mathrm{S}}\right)\right)}{\sin\left(\pi\left(f_{\mathrm{T}}-f_{\mathrm{T}}^{\mathrm{S}}\right)\right)}e^{j2\pi(M-1)\left(f_{\mathrm{T}}-f_{\mathrm{T}}^{\mathrm{S}}\right)}\right] \cdot \\ &\quad \left[\frac{1}{N}\frac{\sin\left(\pi N\left(f_{\mathrm{R}}-f_{\mathrm{R}}^{\mathrm{S}}\right)\right)}{\sin\left(\pi\left(f_{\mathrm{R}}-f_{\mathrm{R}}^{\mathrm{S}}\right)\right)}e^{j2\pi(N-1)\left(f_{\mathrm{R}}-f_{\mathrm{R}}^{\mathrm{S}}\right)}\right], \end{aligned} \tag{7}$$

where $\boldsymbol{u} \triangleq \boldsymbol{b}(f_{\mathrm{R}}) \otimes \boldsymbol{a}(f_{\mathrm{T}})$, $f_{\mathrm{T}} = f_{\mathrm{R}} = \frac{1}{2}\sin(\theta)$, and $\boldsymbol{u}_{\mathrm{S}} \triangleq \boldsymbol{b}(f_{\mathrm{R}}^{\mathrm{S}}) \otimes \boldsymbol{a}\left(f_{\mathrm{T}}^{\mathrm{S}}\right)$.

III. PRC Method to precisely control the 2-D beampattern

In this section, the PRC method is proposed to precisely control the 2-D beampattern in FDA-MIMO radar. We define a rectangular region set $\{\Theta_q\}_{q=1}^{Q}$ and a predefined response set $\{\xi_q\}_{q=1}^{Q}$. In the first stage, multiple artificial interferences with specific JNRs are assigned concurrently within each rectangular region using the iteration algorithm.

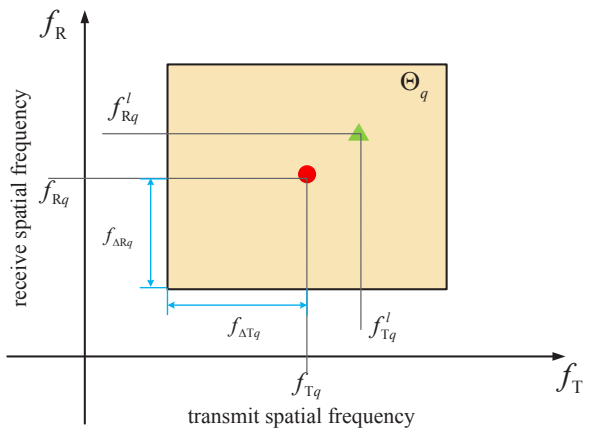

Fig. 1: Artificial interferences within one rectangular region.

Shown in Fig. 1, $f_{\mathrm{T}q}$ and $f_{\mathrm{R}q}$ are respectively defined as the central transmit and receive frequencies of Θ_q. $f_{\Delta\mathrm{T}q}$ and $f_{\Delta\mathrm{R}q}$ denote the transmit and receive frequency scope of Θ_q, respectively. In the l-th ($l \in \mathbb{N}^+$) iteration, the transmit and receive frequencies of the interference are determined by comparing the obtained response with the desired one. For the q-th rectangular region, transmit and receive frequencies of the l-th interference are selected as

$$f^l_{\mathrm{T}q} = \underset{f^i_{\mathrm{T}} \in \Theta_q}{\arg} \left| max\left(P\left(f^i_{\mathrm{T}}, f^i_{\mathrm{R}}\right) - \xi_q\right)\right|, \tag{8a}$$

$$f^l_{\mathrm{R}q} = \underset{f^i_{\mathrm{R}} \in \Theta_q}{\arg} \left| max\left(P\left(f^i_{\mathrm{T}}, f^i_{\mathrm{R}}\right) - \xi_q\right)\right|. \tag{8b}$$

Thus, the jammer-plus-noise covariance matrix is constructed as

$$\boldsymbol{R}^{\{l\}} = \boldsymbol{R}^{\{l-1\}} + \sigma_w^2 \boldsymbol{U}_l \boldsymbol{\Sigma}_l \boldsymbol{U}_l^{\mathrm{H}}, \tag{9}$$

where $\boldsymbol{R}^{\{0\}} = \sigma_w^2 \boldsymbol{I}_{M\times N}$, σ_w^2 denotes the power of the Gaussian distributed noise, $\boldsymbol{\Sigma}_l \triangleq \mathrm{diag}\left\{\frac{\sigma_{l1}^2}{\sigma_w^2}, \frac{\sigma_{l2}^2}{\sigma_w^2}, \cdots, \frac{\sigma_{lQ}^2}{\sigma_w^2}\right\}$ denotes the JNR matrix with σ_{lq}^2 being the power of the interference within the q-th region in the l-th iteration, $\boldsymbol{U}_l = [\boldsymbol{u}_{l1}, \boldsymbol{u}_{l2}, \cdots, \boldsymbol{u}_{lQ}]$ denotes an $MN \times Q$ matrix with $\boldsymbol{u}_{lq} \triangleq \boldsymbol{b}(f^l_{\mathrm{R}q}) \otimes \boldsymbol{a}\left(f^l_{\mathrm{T}q}\right)$ being the steering vector of the interference. The inverse of $\boldsymbol{R}^{\{l\}}$ is written as

$$\begin{aligned}&\left(\boldsymbol{R}^{\{l\}}\right)^{-1} = \left(\boldsymbol{R}^{\{l-1\}}\right)^{-1} \\ &-\left(\boldsymbol{R}^{\{l-1\}}\right)^{-1}\boldsymbol{U}_l\left(\boldsymbol{I}_Q + \sigma_w^2\boldsymbol{\Sigma}_l\boldsymbol{U}_l^{\mathrm{H}}\left(\boldsymbol{R}^{\{l-1\}}\right)^{-1}\boldsymbol{U}_l\right)^{-1} \\ &\cdot\sigma_w^2\boldsymbol{\Sigma}_l\boldsymbol{U}_l^{\mathrm{H}}\left(\boldsymbol{R}^{\{l-1\}}\right)^{-1}.\end{aligned} \tag{10}$$

According to the adaptive theory [18], the weight vector can be obtained as

$$\begin{aligned}&\boldsymbol{w}_l = \Lambda_l\left(\boldsymbol{R}^{\{l\}}\right)^{-1}\boldsymbol{u}_{\mathrm{S}} \\ &= \frac{\boldsymbol{\Gamma}_{l-1}^{\mathrm{H}} - \left(\boldsymbol{R}^{\{l-1\}}\right)^{-1}\boldsymbol{U}_l\left(\boldsymbol{I}_Q + \sigma_w^2\boldsymbol{\Sigma}_l\Upsilon_l\right)^{-1}\sigma_w^2\boldsymbol{\Sigma}_l\boldsymbol{U}_l^{\mathrm{H}}\left(\boldsymbol{R}^{\{l-1\}}\right)^{-1}\boldsymbol{u}_{\mathrm{S}}}{\boldsymbol{\Gamma}_{l-1}\boldsymbol{u}_{\mathrm{S}} - \boldsymbol{\Gamma}_{l-1}\boldsymbol{U}_l\left(\boldsymbol{I}_Q + \sigma_w^2\boldsymbol{\Sigma}_l\Upsilon_l\right)^{-1}\sigma_w^2\boldsymbol{\Sigma}_l\boldsymbol{U}_l^{\mathrm{H}}\left(\boldsymbol{R}^{\{l-1\}}\right)^{-1}\boldsymbol{u}_{\mathrm{S}}},\end{aligned} \tag{11}$$

where $\Upsilon_l = \boldsymbol{U}_l^{\mathrm{H}}\left(\boldsymbol{R}^{\{l-1\}}\right)^{-1}\boldsymbol{U}_l$, $\boldsymbol{\Gamma}_{l-1} = \boldsymbol{u}_{\mathrm{S}}^{\mathrm{H}}\left(\boldsymbol{R}^{\{l-1\}}\right)^{-1}$, and the coefficient is written as

$$\begin{aligned}\Lambda_l &= \left(\boldsymbol{u}_{\mathrm{S}}^{\mathrm{H}}\left(\boldsymbol{R}^{\{l-1\}}\right)^{-1}\boldsymbol{u}_{\mathrm{S}}\right)^{-1} \\ &= \left[\begin{array}{l}\boldsymbol{u}_{\mathrm{S}}^{\mathrm{H}}\left(\boldsymbol{R}^{\{l-1\}}\right)^{-1}\boldsymbol{u}_{\mathrm{S}} - \boldsymbol{u}_{\mathrm{S}}^{\mathrm{H}}\left(\boldsymbol{R}^{\{l-1\}}\right)^{-1}\boldsymbol{U}_l\left(\boldsymbol{I}_Q\right. \\ \left.+\boldsymbol{S}_l\boldsymbol{U}_l^{\mathrm{H}}\left(\boldsymbol{R}^{\{l-1\}}\right)^{-1}\boldsymbol{U}_l\right)^{-1}\boldsymbol{S}_l\boldsymbol{U}_l^{\mathrm{H}}\left(\boldsymbol{R}^{\{l-1\}}\right)^{-1}\boldsymbol{u}_{\mathrm{S}}\end{array}\right]^{-1}.\end{aligned} \tag{12}$$

With a predefined response ξ_q at $\boldsymbol{u}_{lq}$, the normalized transmit-receive 2-D beampattern which is pointed at $\boldsymbol{u}_{\mathrm{S}}$ and evaluated at $\boldsymbol{u}_{lq}$ is written as

$$P\left(\boldsymbol{u}_{lq}\left|\boldsymbol{u}_{\mathrm{S}}\right.\right) = \boldsymbol{w}_l^{\mathrm{H}}\boldsymbol{u}_{lq} = \xi_q. \tag{13}$$

Substituting (11) into (13), the response of the beampattern at $\boldsymbol{u}_{lq}$ with a predefined response ξ_q is derived as follows

$$\begin{aligned}&P\left(\boldsymbol{u}_{lq}\left|\boldsymbol{u}_{\mathrm{S}}\right.\right) = \boldsymbol{w}_l^{\mathrm{H}}\boldsymbol{u}_{lq} = \xi_q \\ &= \frac{\boldsymbol{\Gamma}_{l-1}\boldsymbol{u}_{lq} - \boldsymbol{\Gamma}_{l-1}\boldsymbol{U}_l(\boldsymbol{I}_Q + \boldsymbol{S}_l\Upsilon_l)^{-1}\boldsymbol{S}_l\boldsymbol{U}_l^{\mathrm{H}}\left(\boldsymbol{R}^{\{l-1\}}\right)^{-1}\boldsymbol{u}_{lq}}{\boldsymbol{\Gamma}_{l-1}\boldsymbol{u}_{\mathrm{S}} - \boldsymbol{\Gamma}_{l-1}\boldsymbol{U}_l(\boldsymbol{I}_Q + \boldsymbol{S}_l\Upsilon_l)^{-1}\boldsymbol{S}_l\boldsymbol{U}_l^{\mathrm{H}}\left(\boldsymbol{R}^{\{l-1\}}\right)^{-1}\boldsymbol{u}_{\mathrm{S}}},\end{aligned} \tag{14}$$

where $\boldsymbol{S}_J \triangleq \sigma_w^2\boldsymbol{\Sigma}_J$. The equation is further expressed as

$$\begin{aligned}&\boldsymbol{\Gamma}_{l-1}\boldsymbol{U}_l(\boldsymbol{I}_Q + \boldsymbol{S}_l\Upsilon_l)^{-1}\boldsymbol{S}_l\boldsymbol{U}_l^{\mathrm{H}}\left(\boldsymbol{R}^{\{l-1\}}\right)^{-1}(\xi_q\boldsymbol{u}_{\mathrm{S}} - \boldsymbol{u}_{lq}) \\ &= \boldsymbol{\Gamma}_{l-1}\xi_q\boldsymbol{u}_{\mathrm{S}} - \boldsymbol{\Gamma}_{l-1}\boldsymbol{u}_{lq}.\end{aligned} \tag{15}$$

As there are Q regions to be precisely controlled, we can further form an equation by collecting Q responses, i.e., $P\left(\boldsymbol{u}_{l1}\left|\boldsymbol{u}_{\mathrm{S}}\right.\right) = \xi_1, P\left(\boldsymbol{u}_{l2}\left|\boldsymbol{u}_{\mathrm{S}}\right.\right) = \xi_2, \cdots, P\left(\boldsymbol{u}_{lQ}\left|\boldsymbol{u}_{\mathrm{S}}\right.\right) = \xi_Q$. Define a $Q \times Q$ matrix $\boldsymbol{Y}_l \triangleq \boldsymbol{U}_l^{\mathrm{H}}\left(\boldsymbol{R}^{\{l-1\}}\right)^{-1}\left(\boldsymbol{u}_{\mathrm{S}}\boldsymbol{\xi}^{\mathrm{T}} - \boldsymbol{U}_l\right)$ with $[\boldsymbol{Y}_l]_{:,q} = \boldsymbol{U}_l^{\mathrm{H}}\left(\boldsymbol{R}^{\{l-1\}}\right)^{-1}(\xi_q\boldsymbol{u}_{\mathrm{S}} - \boldsymbol{u}_{lq})$, $\boldsymbol{\xi} \triangleq [\xi_1, \xi_2, \cdots, \xi_Q]^{\mathrm{T}}$, $\boldsymbol{\eta}_l \triangleq \boldsymbol{\Gamma}_{l-1}\boldsymbol{u}_{\mathrm{S}}\boldsymbol{\xi}^{\mathrm{T}} - \boldsymbol{\Gamma}_{l-1}\boldsymbol{U}_l$ with $[\boldsymbol{\eta}_l]_q = \xi_q\boldsymbol{\Gamma}_{l-1}\boldsymbol{u}_{\mathrm{S}} - \boldsymbol{\Gamma}_{l-1}\boldsymbol{u}_{lq}$. The equation is expressed as

$$\boldsymbol{\Gamma}_{l-1}\boldsymbol{U}_l(\boldsymbol{I}_Q + \boldsymbol{S}_l\Upsilon_l)^{-1}\boldsymbol{S}_l\boldsymbol{Y} = \boldsymbol{\eta}_l. \tag{16}$$

Since $\boldsymbol{S}_l$, Υ_l, and $\boldsymbol{Y}$ are all $L \times L$ full-rank matrices, the matrix $(\boldsymbol{I}_Q + \boldsymbol{S}_l\Upsilon_l)^{-1}\boldsymbol{S}_l\boldsymbol{Y}_l$ is a nonsingular matrix. Multiplying $\left[(\boldsymbol{I}_Q + \boldsymbol{S}_l\Upsilon_l)^{-1}\boldsymbol{S}_l\boldsymbol{Y}_l\right]^{-1}$ to both sides of the equation simultaneously, (16) is written as

$$\boldsymbol{\Gamma}_{l-1}\boldsymbol{U}_l - \boldsymbol{\eta}_l\boldsymbol{Y}_l^{-1}\Upsilon_l = \boldsymbol{\eta}_l\boldsymbol{Y}_l^{-1}\boldsymbol{S}_l^{-1}. \tag{17}$$

As $\boldsymbol{S}_l$ is a diagonal matrix, the JNR of the q-th interference is calculated as

$$[\boldsymbol{\Sigma}_l]_{q,q} = \frac{[\boldsymbol{S}_l]_{q,q}}{\sigma_w^2} = \frac{\sigma_{lq}^2}{\sigma_w^2} = \frac{\left[\boldsymbol{\eta}_l\boldsymbol{Y}_l^{-1}\right]_q}{\sigma_w^2\left[\boldsymbol{\Gamma}_{l-1}\boldsymbol{U}_l - \boldsymbol{\eta}_l\boldsymbol{Y}_l^{-1}\Upsilon_l\right]_q}. \tag{18}$$

Notably, only the response of the temporarily imposed interference can be precisely controlled in each iteration, however, the previously-controlled responses may have some perturbations. Thus, if the response requirement of one region is satisfied, in the second stage, only a small amount of extra artificial interferences are imposed successively within the remaining regions in order to guarantee the predefined responses for all regions.

Take the q-th region for example, the jammer-plus-noise

covariance matrix in the k-th($k \in \mathbb{N}^+$) iteration is updated as

$$\boldsymbol{R}^{\{k\}} = \boldsymbol{R}^{\{k-1\}} + \sigma_k^2 \boldsymbol{u}_k \boldsymbol{u}_k^{\mathrm{H}}, \tag{19}$$

where the initial matrix $\boldsymbol{R}^{\{0\}} = \boldsymbol{R}^{\{l\}}$ is calculated using (9). According to $P(\boldsymbol{u}_k | \boldsymbol{u}_{\mathrm{S}}) = \xi_q$, that is

$$P(\boldsymbol{u}_k | \boldsymbol{u}_{\mathrm{S}}) = \xi_q = \frac{\boldsymbol{u}_S^{\mathrm{H}} \left(\boldsymbol{R}^{\{k-1\}}\right)^{-1} \boldsymbol{u}_k \Upsilon - \sigma_k^2 \boldsymbol{u}_S^{\mathrm{H}} \left(\boldsymbol{R}^{\{k-1\}}\right)^{-1} \boldsymbol{u}_k \boldsymbol{u}_k^{\mathrm{H}} \left(\boldsymbol{R}^{\{k-1\}}\right)^{-1} \boldsymbol{u}_k}{\boldsymbol{u}_S^{\mathrm{H}} \left(\boldsymbol{R}^{\{k-1\}}\right)^{-1} \boldsymbol{u}_S \Upsilon - \sigma_k^2 \boldsymbol{u}_S^{\mathrm{H}} \left(\boldsymbol{R}^{\{k-1\}}\right)^{-1} \boldsymbol{u}_k \boldsymbol{u}_k^{\mathrm{H}} \left(\boldsymbol{R}^{\{k-1\}}\right)^{-1} \boldsymbol{u}_S}, \tag{20}$$

where $\Upsilon \triangleq 1 + \sigma_k^2 \boldsymbol{u}_k^{\mathrm{H}} \left(\boldsymbol{R}^{\{k-1\}}\right)^{-1} \boldsymbol{u}_k$. Then, the power of interference from the q-th rectangular region in the k-th iteration is calculated as

$$\sigma_k^2 = \frac{1}{\xi_q \boldsymbol{u}_S^{\mathrm{H}} \left(\boldsymbol{R}^{\{k-1\}}\right)^{-1}} \cdot \frac{\boldsymbol{u}_S^{\mathrm{H}} \left(\boldsymbol{R}^{\{k-1\}}\right)^{-1} (\boldsymbol{u}_k - \xi \boldsymbol{u}_S)}{\left[\boldsymbol{u}_S \boldsymbol{u}_k^{\mathrm{H}} \left(\boldsymbol{R}^{\{k-1\}}\right)^{-1} \boldsymbol{u}_k - \boldsymbol{u}_k \boldsymbol{u}_k^{\mathrm{H}} \left(\boldsymbol{R}^{\{k-1\}}\right)^{-1} \boldsymbol{u}_S\right]}, \tag{21}$$

By imposing extra artificial interferences within each rectangular region, the response levels can be successively adjusted until the predefined response control requirement is satisfied for all regions. Finally, the developed PRC method in the FDA-MIMO radar is summarized in Algorithm 1.

Algorithm 1 PRC Algorithm

1. Give Q, $\{\Theta_q\}_{q=1}^Q$, $\{f_{\mathrm{T}q}\}_{q=1}^Q$, $\{f_{\mathrm{R}q}\}_{q=1}^Q$, $\{\beta_q\}_{q=1}^Q = \infty$, $\{\xi\}_{q=1}^Q$, $\boldsymbol{u}_S$, $\boldsymbol{U}_l$, $\boldsymbol{R}^{\{0\}} = \sigma_w^2 \boldsymbol{I}_{M\times N}$, σ_w^2, $l = 1$, $k = 1$;

while $\min_q \{\beta_q\} > \beta_\varepsilon$ **do**

2. Select $f_{\mathrm{T}q}^l$ and $f_{\mathrm{R}q}^l$ according to (8);
3. Calculate $\frac{\sigma_{lq}^2}{\sigma_w^2}$ using (18) and obtain $\boldsymbol{\Sigma}_l = \mathrm{diag}\left\{\frac{\sigma_{l1}^2}{\sigma_w^2}, \frac{\sigma_{l2}^2}{\sigma_w^2}, \cdots, \frac{\sigma_{lQ}^2}{\sigma_w^2}\right\}$;
4. Update $\boldsymbol{R}^{\{l\}} = \boldsymbol{R}^{\{l-1\}} + \sigma_w^2 \boldsymbol{U}_l \boldsymbol{\Sigma}_l \boldsymbol{U}_l^{\mathrm{H}}$;
5. Update $\boldsymbol{w}_l = \Lambda_l \left(\boldsymbol{R}^{\{l\}}\right)^{-1} \boldsymbol{u}_{\mathrm{S}}$ using (11);
6. Obtain $\beta_q = \max_q \{P(\Theta_q | \boldsymbol{u}_{\mathrm{S}}) - \xi_q\}$;
7. $l = l + 1$;

end while

8. Select the remaining $\{\Theta_q\}_{q=1, q\neq q_*}^Q$ to add extra artificial interferences;

while $\beta_q > \beta_\varepsilon$ **do**

9. Select $f_{\mathrm{T}q}^k$ and $f_{\mathrm{R}q}^k$ according to (8);
10. Calculate σ_k^2 according to (21);
11. Update $\boldsymbol{R}^{\{k\}} = \boldsymbol{R}^{\{k-1\}} + \sigma_k^2 \boldsymbol{u}_k \boldsymbol{u}_k^{\mathrm{H}}$;
12. $k = k + 1$;

end while

13. **Output**: weight vector $\boldsymbol{w}_{\mathrm{FINAL}} = \left(\boldsymbol{u}_{\mathrm{S}}^{\mathrm{H}} \left(\boldsymbol{R}^{\{k-1\}}\right)^{-1} \boldsymbol{u}_{\mathrm{S}}\right)^{-1} \left(\boldsymbol{R}^{\{k\}}\right)^{-1} \boldsymbol{u}_{\mathrm{S}}$.

IV. Simulation Results

In this section, simulations are performed to verify the effectiveness of the proposed PRC algorithm to precisely control the transmit-receive 2-D beampattern in FDA-MIMO radar. Simulation parameters are listed in Table 1.

TABLE I: Simulation Parameters

Parameter	Value
carrier frequency	10GHz
$N = M$	10
Frequency increment	3750Hz
wavelength	0.03m
PRF	5000Hz
Q	3
$\{\xi_q\}_{q=1}^Q$	$\{0.0018, 0.01, 0.0005\}$
$\{f_{\Delta \mathrm{T}q}\}_{q=1}^Q$	$\{0.05, 0.1, 0.05\}$
$\{f_{\Delta \mathrm{R}q}\}_{q=1}^Q$	$\{0.5, 0.1, 0.1\}$
$\{f_{\mathrm{T}q}\}_{q=1}^Q$	$\{0.25, -0.25, -0.375\}$
$\{f_{\mathrm{R}q}\}_{q=1}^Q$	$\{0, -0.25, 0\}$
β_ε	0.0005
$f_{\mathrm{T}}^{\mathrm{S}}$	0
$f_{\mathrm{R}}^{\mathrm{S}}$	0

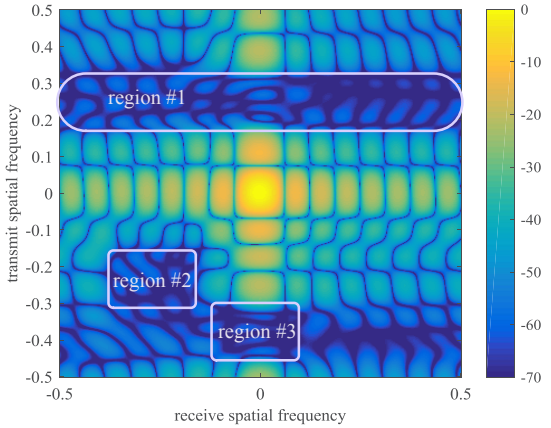

(a)

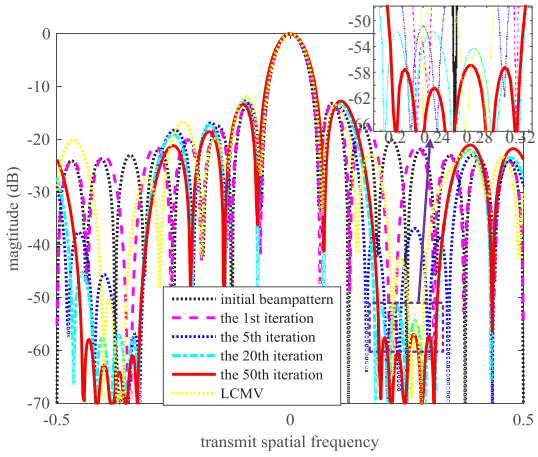

(b)

Fig. 2: Precise response of transmit-receive 2-D beampattern. (a) Beampattern with controlled regions. (b) Equivalent transmit beampattern at $f_R = 0$.

Fig.2 illustrates the resultant transmit-receive 2-D beampattern with the PRC algorithm. We consider a notch with -55dB, two null regions with -60dB and -66dB, respectively. It is seen from Fig. 2 (a) that the beampattern with precisely controlled response is formed in the joint transmit-receive spatial frequency domain. The responses in region #1 are low and the null depths for region #2 and region #3 are deep. Fig. 2 (b) shows the beampatterns of the proposed algorithm at $f_{\mathrm{R}} = 0$ for different iterations. It can be seen that the responses of region #1 and region #3 decrease with the increase of iterations. Notice that the response level is lower than the desired one because the previously-controlled responses may have some perturbations. Moreover, we compare the PRC algorithm with the linearly constrained minimum variance (LCMV) beamformer where several linear constraints are imposed when minimizing the output variance [19]. As we can see, the PRC method outperforms the LCMV beamformer.

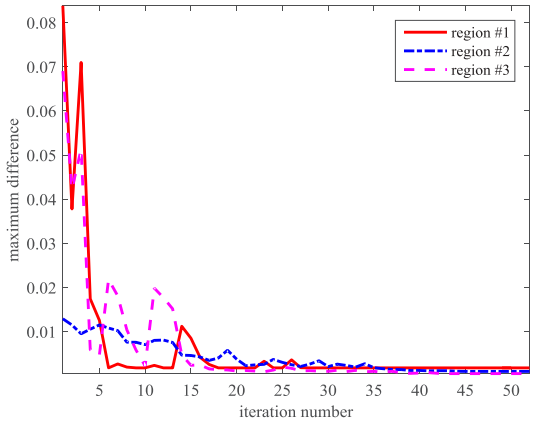

Fig. 3: Maximum difference of the resultant beampattern and the predefined value versus number of iterations.

Fig. 3 demonstrates the maximum difference of the resultant beampattern and the predefined value for different regions. Monte Carlo experiments with 200 trials are carried out. It can be seen that the values of differences for region #1 and region #3 drop rapidly after about 10 iterations. It means the proposed PRC algorithm features high speed of convergence.

V. Conclusions

In this paper, the response of the transmit-receive 2-D beampattern in FDA-MIMO radar was precisely controlled via jammer-plus-noise covariance matrix construction. Subsequently, the weight vector was updated to achieve the desired response. The algorithm was firstly performed by concurrently imposing artificial interferences within rectangular regions in the joint transmit-receive spatial frequency domain. In the second stage, extra artificial interferences were added to satisfy the response requirement for all regions. In particular, closed-form expressions of the JNRs of artificial interferences were given.

With the proposed method, a 2-D beampattern with low sidelobe levels and broadened deep nulls in precisely controlled rectangular regions is formed. It can be applied to jammer suppression where the range and angle of the interference are time-varying.

Acknowledgment

This work was supported in part by the National Nature Science Foundation of China under Grant 61621005.

References

[1] J. Li and P. Stoica, Robust Adaptive Beamforming. New York: Wiley, 2006.
[2] X. Zhang, Z. He, B. Liao, X. Zhang, and W. Peng, 'Pattern synthesis for arbitrary arrays via weight vector orthogonal decomposition,' *IEEE Trans. Signal Process.*, vol. 66, no. 5, pp.1286-1299, Mar. 2018.
[3] P. Y. Zhou and M. A. Ingram, 'Pattern synthesis for arbitrary arrays using an adaptive array method,' *IEEE Trans. Antennas Propag.*, vol. 47, no. 5, pp. 862-869, May 1999.
[4] K. K. Yan and Y. Lu, 'Sidelobe reduction in array-pattern synthesis using genetic algorithm,' *IEEE Trans. Antennas Propag.*, vol. 45, no. 7, pp. 1117-1122, Jul. 1997.
[5] D. W. Boeringer and D. H. Werner, 'Particle swarm optimization versus genetic algorithms for phased array synthesis,' *IEEE Trans. Antennas Propag.*, vol. 52, no. 3, pp. 771-779, Mar. 2004.
[6] V. Murino, A. Trucco, and C. S. Regazzoni, 'Synthesis of unequally spaced arrays by simulated annealing,' *IEEE Trans. Signal Process.*, vol. 44, no. 1, pp. 119-122, Jan. 1996.
[7] B. Fuchs, 'Application of convex relaxation to array synthesis problems,' *IEEE Trans. Antennas Propag.*, vol. 62, pp. 634-640, 2014.
[8] C. A. Olen and R. T. Compton Jr., 'A numerical pattern synthesis algorithm for arrays,' *IEEE Trans. Antennas Propag.*, vol. 38, pp. 1666-1676, 1990.
[9] X. Zhang, Z. He, X.-G. Xia, B. Liao, X. Zhang, and Y. Yang, 'OPARC: Optimal and Precise Array Response Control Algorithm-Part I: Fundamentals,' *IEEE Trans. Signal Process.*, vol. 67, no. 3, pp. 652-667, 2019.
[10] P. Antonik, M. C.Wicks, H. D. Griffths, and C. J. Baker, 'Frequency diverse array radars,' in: Proceedings of the IEEE Radar Conference, Verona, NY, USA, April 2006, pp. 215-217.
[11] J. Xu, S. Zhu, and G. Liao,'An adaptive range-angle-Doppler processing approach for FDA-MIMO radar using three-dimensional localization,' *IEEE J. of Sel. Topics in Signal Process.*, vol. 11, no. 2, pp. 309-320.
[12] J. Xiong, W.-Q. Wang, and K. Gao, 'FDA-MIMO radar range-angle estimation: CRLB, MSE, and resolution analysis,' *IEEE Trans. Aerosp. Electron. Syst.*, vol. 54, no. 1, p. 284-294, 2018.
[13] A. Basit, W. Khan, S. Khan, and I. M. Qureshi, 'Development of frequency diverse array radar technology: a review,' *IET Radar, Sonar Navigat.*, vol. 12, no. 2, pp. 165-175, 2018.
[14] W.-Q. Wang, 'Overview of frequency diverse array in radar and navigation applications,' *IET Radar, Sonar Navigat.,* vol. 10, no. 6, pp.1001-1012, 2016.
[15] C. Wen, J. Peng, Y. Zhou, and J. Wu, 'Enhanced three-dimensional joint domain localized STAP for airborne FDA-MIMO radar under dense false-target jamming scenario,' IEEE Sensors J., vol. 8, no. 10, pp. 4154-4166, 2018.
[16] L. Lan, G. Liao, J. Xu, Y. Zhang, and F. Fioranelli, 'Suppression approach to main-beam deceptive jamming in FDA-MIMO radar using nonhomogeneous sample detection,' *IEEE Access*, vol. 6, no. 1, pp. 34582-34597, 2018.
[17] J. Xu, G. Liao, S. Zhu, L. Huang, and H. C. So, 'Joint range and angle estimation using MIMO radar with frequency diverse array,' *IEEE Trans. Signal Process.*, vol. 63, no. 13, pp. 3396-3410, 2015.
[18] H. K. Van Trees, Optimum Array Processing. New York: Wiley, 2002.
[19] O. L. Frost, 'An algorithm for linearly constrained adaptive array processing,' *Proc. IEEE*, vol. 60, pp. 926-935, 1972.